**Proceedings of the ASME 2017 International Design Engineering Technical Conference &
13th International Conference on Multibody Systems, Nonlinear Dynamics, and Control
IDETC/ MSNDC 2017
August 6-9, 2017, Cleveland, OH, USA**

DRAFT: DETC2017-67859

PREDICTING DAMPING OF A CANTILEVER BEAM WITH A BOLTED JOINT USING QUASI-STATIC MODAL ANALYSIS

Emily A. Jewell
Undergraduate Student
Engineering Mechanics Program
University of Wisconsin-Madison
534 Engineering Research Building
1500 Engineering Drive
Madison, Wisconsin 53706
ejewell@wisc.edu

Matthew S. Allen
Associate Professor
Department of Engineering Physics
University of Wisconsin-Madison
535 Engineering Research Building
1500 Engineering Drive
Madison, Wisconsin 53706
msallen@engr.wisc.edu

Robert Lacayo
Graduate Student
Engineering Mechanics Program
University of Wisconsin-Madison
534 Engineering Research Building
1500 Engineering Drive
Madison, Wisconsin 53706
lacayo@wisc.edu

ABSTRACT

Bolted joints are common in assembled structures and are a large contributor to the damping in these assemblies. The joints can cause the structure to behave nonlinearly, and introduce uncertainty because the effective stiffness and damping at the joint are typically unknown. Consequently, improved modeling methods are desired that will address the nonlinearity of the jointed structured while also providing reasonable predictions of the effective stiffness and damping of the joint as a function of loading.

A method proposed by Festjens, Chevallier and Dion addresses this by using a sort of nonlinear modal analysis based on the response of the structure to quasi-static loading. This was further developed by Allen and Lacayo and thoroughly demonstrated for structures with discrete Iwan joints. This work explores the efficacy of quasi-static modal analysis for 2D and 3D finite element models in which the geometry, contact pressure and friction in the joint are modeled in detail. The mesh density, contact laws, and other solver settings are explored to understand what is needed to obtain convergence for this type of problem. For the 2D case study, the effect of bolt preload and coefficient of friction are explored and shown to produce reasonable trends. Three dimensional models prove far more challenging and significant effort was required to obtain convergence and then to obtain results that are physically realistic; these efforts are reported as well as the lessons learned.

INTRODUCTION

Finite element analysis is the cornerstone of modern day structural analysis. From rollercoasters to rovers, FEA allows for the discretization of a CAD model into a mesh of nodes and elements from which a variety of analyses can be performed to examine the structure's stresses, thermal loading, vibrational modes, and more. Current FEA methods produce extremely accurate results for models of a single solid and often rely on linear solvers to do so. Most structures, however, are composed of multiple parts fastened together and it is not straightforward to determine the effective stiffness and damping of these connections [1]. Furthermore, the modeled connections introduce nonlinearities that can make the model very costly to simulate, and may require expensive physical prototype tests to validate [2-7].

To help address this, Festjens et al. [8] proposed a model reduction technique that spatially decomposes a structure into a linear domain away from the joint and a nonlinear domain near the joint. Then the inertial term in the joint domain is neglected and the joint is assumed to behave quasi-statically. Allen et al. [9] later presented a variant on this method and applied it to structures where the joints were modeled as discrete Iwan elements. Their work demonstrated that the technique produces very accurate estimates of the amplitude-dependent modal damping and natural frequency when the response is dominated by a single mode, thus allowing them to more easily tune Iwan models to reproduce the nonlinear damping (and to a lesser extent stiffness) observed in experiments. In essence, the developed quasi-static modal analysis is an extension of modal analysis to structures with weakly nonlinear joints.

The Iwan models used in [9] are not predictive but need to be tuned to experimental measurements for every joint geometry, preload, material, etc… In contrast, this work explores the use of quasi-static modal analysis to predictive modeling of a joint wherein the joint geometry, bolt preload force, and interface

friction law are used to predict the nonlinear behavior of each mode.

To effectively model a bolted joint, it is important to first take a step back and understand the mechanics of a bolted interface; several phenomena occur when two members are fastened together. First, the bolt itself imposes a clamping force proportional to the bolt preload on the joined members, forcing them into contact with one another. Simultaneously, friction limits lateral motion of the surfaces. Then, if the bolted structure has external forces applied, these effects will result in the bolted surfaces trying to slip relative to each other. First the bolted contacting members will experience microslip, or slipping near the edge of contact where the clamping pressure is lowest. As the external forces increase in magnitude though, the joint may slip completely and transition from microslip to macroslip. In the macroslip regime, severe nonlinearity can be observed.

Microslip is known to cause damping, up to 90% of the damping in some systems [10], and can induce fatal fretting fatigue [11]. However, it is costly to model and so microslip is typically neglected in FE models. Instead, an iterative method is used in which a FE model of the structure is created and a physical prototype is constructed. Then tests are conducted on the prototype to estimate the structure's damping, and then the measured damping is imposed on the linear FE model. This process is repeated until the model is deemed acceptable for structural dynamic response prediction.

In addition to the existing analysis methods being extremely costly, various studies have shown that structures with bolted joints can exhibit variations in damping of hundreds of percent with response amplitude. Therefore the existing analysis method may not provide tractable results to the structures life cycle and thus a more robust and predictive method for modeling joints is needed [12-17]. To address the latter of these concerns, any method to examine damping in a built up structure should assess a variety of forcing magnitudes. For the quasi-static method employed in this paper, this was done by imposing a range of load levels, or forcing magnitudes, on the models which allowed for energy dissipation analysis over most of the microslip regime with maximum forcing levels near the initiation of macroslip.

The friction responsible for the joint's microslip and macroslip was modeled by Coulomb friction in this work. There is a current discussion in regards to the effectiveness of assuming a Coulomb friction model and whether it is sufficient for contact mechanics [18-20]. Coulomb friction is often used for mechanical contact problems, and while it has often proved effective when modeling macroslip, there is evidence that it is not adequate for microslip [21]. Adam Brink's thesis examined this concern and concluded that with proper solver settings for the FEA model, Coulomb friction is still acceptable for microslip models [22]. However, because bolted joints are so costly to model, only one study has ever thoroughly compared experimental measurements of dissipation with detailed contact simulations [6]. The tools developed in this work could be used to rigorously characterize the effect of the friction law on the nonlinear damping of each mode in a structure.

Lastly, as advanced, lightweight structures are being developed, passive vibration reduction has become increasingly important for design. Since bolted joints usually do provide increased damping, they may be designed in structures of the future as a form of vibration reduction, assuming the damping created by the joints and resulting from microslip may be suitably modeled [23]. It is therefore hoped that the methods presented here will one day allow accurate and efficient simulation of microslip and joint energy dissipation, so designers can exploit this to maximize damping.

In summary, the aim of this work is to implement the quasi-static modal analysis method for structures where the joint is modeled in detail, and to assess its accuracy and effectiveness. First a 2D model was examined in Abaqus since its smaller size and simple mesh allowed for fast computation. Several iterations were performed to determine what mesh was needed to obtain convergence in the quasi-static calculations of damping. Once a converged model had been obtained, the bolt preload and coefficient of friction were varied in order to understand how these parameters affect the instantaneous frequency and damping of the first bending mode. These types of parameter studies will be needed in future studies when predictions are compared with measurements of damping versus amplitude. The insights gained from the 2D model then guided the analysis for the 3D model, where case studies were performed to determine ideal Abaqus model settings to obtain a simulation that produces reliable results.

REVIEW OF THE QUASI-STATIC MODAL ANALYSIS METHOD

The quasi-static modal analysis method implemented in this paper is similar to one developed by Festjens, Chevallier, and Dion [8] where the effective natural frequency and modal damping ratios can be extracted from a structure. This is done by imposing a quasi-static load to the model that would excite only a single mode of the linearized structure. Allen and Lacayo [9] recently elaborated on this method, and used the modal load-displacement curves to construct a hysteresis curve which allowed for effective frequency and energy dissipation estimations.

Consider the equation of motion for a structure with a joint, which can be written as,

$$\mathbf{M}\ddot{\mathbf{x}} + \mathbf{C}\dot{\mathbf{x}} + \mathbf{K}\mathbf{x} + \mathbf{f}_J(\mathbf{x}, \boldsymbol{\theta}) = \mathbf{f}_{ext}(t) \tag{1}$$

where $\mathbf{M}$, $\mathbf{C}$, and $\mathbf{K}$ are, respectively, the mass, damping, and stiffness matrices of the system, and $\mathbf{x}$, $\dot{\mathbf{x}}$, and $\ddot{\mathbf{x}}$ are the displacement, velocity, and acceleration vectors, respectively. The vector $\mathbf{f}_J$ represents the internal forces due to a joint model containing internal sliders, and $\boldsymbol{\theta}$ is a vector that captures the state (slip or stick) of each slider element.

At low amplitudes the joints can be replaced with springs equivalent to the zero-load equilibrium stiffness of the joints,

$$\mathbf{K}_T = \left.\frac{\partial \mathbf{f}_J}{\partial \mathbf{x}}\right|_{\mathbf{x}=\mathbf{0}} \tag{2}$$

and an eigenvalue problem can be solved to estimate the mass-normalized mode shapes, φ_r , of the structure.

$$\left(\left[\mathbf{K}+\mathbf{K}_T\right]-\lambda_r\mathbf{M}\right)\boldsymbol{\varphi}_r=\mathbf{0} \quad . \tag{3}$$

A force $\mathbf{f}_{\text{ext}}=\mathbf{M}\boldsymbol{\varphi}_r$ is applied which distributes a load over the entire structure such that only mode *r* of the system would respond if the structure were linear. Using the approach in [8, 9], this force is applied to the nonlinear model resulting in the following quasi-static problem,

$$\mathbf{K}\mathbf{x}+\mathbf{f}_J(\mathbf{x},\boldsymbol{\theta})=\mathbf{M}\boldsymbol{\varphi}_r\alpha \tag{4}$$

where α is a scalar which sets the load amplitude. A finite element package returns the response, $\mathbf{x}(\alpha)$, which can then be mapped onto the *r*th mode using:

$$q_r(\alpha)=\boldsymbol{\varphi}_r{}^{\mathrm{T}}\mathbf{M}\mathbf{x}(\alpha) \tag{5}$$

One can also compute the amplitude of modes other than the one in question to determine whether modal coupling is important at each load amplitude.

Using this approach, the hysteresis curve can be constructed from a single, quasi-static ramp-up loading from 0 to α if the nonlinear forces are independent of the velocity and if each mode obeys the Masing assumptions [5, 8]. The modal force is then given by

$$f_r(\alpha)=\boldsymbol{\varphi}_r{}^{\mathrm{T}}\mathbf{M}\boldsymbol{\varphi}_r\alpha=\alpha\,. \tag{6}$$

Then using Masing's rules, the force (and similarly displacement) over a full loading cycle can be estimated yielding the following forward and reverse curves.

$$\begin{aligned}\hat{f}_1(q_r)&=2f_r\left(\tfrac{q_r+q_r(\alpha)}{2}\right)-\alpha\\ \hat{f}_2(q_r)&=\alpha-2f_r\left(\tfrac{q_r(\alpha)-q_r}{2}\right)\end{aligned}\quad . \tag{7}$$

The secant of this hysteresis curve is then used to estimate the instantaneous natural frequency of the mode in question:

$$\omega_r(\alpha)=\sqrt{\frac{\alpha}{q_r(\alpha)}} \tag{8}$$

The energy dissipated for each vibration cycle is the area under the hysteresis curve,

$$\begin{aligned}D_r(\alpha)&=\int_{-q_r(\alpha)}^{q_r(\alpha)}\left(\hat{f}_1(q_r)-\hat{f}_2(q_r)\right)dq_r\\&=2\int_{-q_r(\alpha)}^{q_r(\alpha)}\left(f_r\left(\tfrac{q_r+q_r(\alpha)}{2}\right)+f_r\left(\tfrac{q_r(\alpha)-q_r}{2}\right)-\alpha\right)dq_r\end{aligned} \tag{9}$$

The integral above is readily evaluated using the trapezoid rule and then the effective damping ratio $\zeta_r(\alpha)$ may be determined by analogy with a linear system. See [3,5] for further details.

$$\zeta_r(\alpha)=\frac{D(\alpha)}{2\pi\left(q_r(\alpha)\omega_r(\alpha)\right)^2} \tag{10}$$

The damping is typically small and so little hysteresis is visible. When plotting the hysteresis curves, it is helpful to plot only the nonlinear part, which is given by the following. For example, see Fig. 3.

$$\hat{f}_1(q_r)_{NL}=\hat{f}_1(q_r)-q_r\omega_{0r}{}^2 \tag{11}$$

APPLICATION TO 2D MODEL

Finite Element Model Creation

To begin, a 2D model of stacked cantilever beams with a bolted joint was constructed in Abaqus. Each beam was 203 mm [8 in] long, 6.35 mm [0.25 in] thick and assumed infinite in width due to the selection of plane strain CPE4 elements. A fixed boundary condition was applied to one end of the structure. The bolt was modeled by a line pressure load on both the top and bottom faces of the stacked beams in a 6.35 mm [0.25 in] wide section 25.4 mm [1 in] from the free end of the structure. A pressure of 288 Nm [2546 lb-in] was applied on each segment, corresponding to the clamping pressure applied by a 6.35 mm [0.25 in] diameter bolt with 4450 N [1000 lb] of preload split between the top and bottom surfaces.

Both the bolt and beams were made of steel with material properties E = 200 GPa [2.9e7psi], υ = 0.285, and ρ =6600 kg/m³ [7.34e-3 slugs/in³]. The material was linear elastic so that the only damping in the model came from Coulomb friction and material damping was neglected since it can be readily added after the analysis if need be.

The structure was then meshed in Abaqus with smaller elements around the bolt and washer regions which were expected to experience microslip. To reduce computational costs, larger elements were used towards the fixed boundary condition where minimal motion was expected. The final mesh used for quasi-static analysis is shown in Fig. 1 where the elements are colored to highlight key regions within the model. The meshed assembly ultimately consisted of two idenitically meshed beams duplicated atop one another.

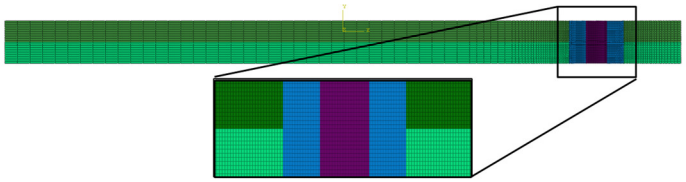

Figure 1. Finite element model of 2D bolted structure model composed of top beam (dark green), bottom beam (light green), bolt region with pressure line loads (maroon), and washer region (blue).

When initially creating the finite element mesh, elements were sized following the typical process for stress analysis which resulted in approximately 10 elements across the bolt and washer contact regions. However, after performing a few quasi-static analyses on the model, it was discovered that microslip was not being captured and that the model was instead jumping into macroslip. Re-examining the importance of element size surrounding the bolt, the work by Brink [22] was found to suggest 120 elements over the region of contact, and so the mesh was drastically refined and subsequently found to be adequate. A

mesh convergence study was then performed to verify these results, as documented in a later subsection.

Next, contact was enabled along the full length of the beams with a coefficient of friction $\mu = 0.6$ [24]. Abaqus allows several methods for addressing the tangential and normal behavior of contact, where the default method is a Penalty method in both directions. Work by Daniel Segalman and Adam Brink in [6, 22] suggested changing the tangential formulation to the Lagrange Multiplier method while maintaining the default hard contact (Penalty) method for normal behavior, so these formulations were implemented on the 2D model. These formulations were later revisited in detail for the 3D model.

To verify the efficacy of this change to the tangential contact formulation, a comparison of quasi-static modal analysis results for the energy dissipation in the joint was done on the 2D model with either the Lagrange or Penalty method tangential contact formulation. Both methods gave nearly identical solve times and results in 2D, suggesting the Lagrange method is a suitable tangential contact selection when trying to capture microslip at the joint. These results, comparing Lagrange and Penalty methods, were in agreement with conclusions drawn in [6] where it was found both methods may give accurate results but the Lagrange formulation is preferred since the Penalty method requires an extensive trial and error process of adjusting the slip tolerance and FEM.

Quasi-static Analysis Results

After creating the finite element model, the quasi-static analysis method was implemented. A two-step analysis was performed that first imposed the bolt preload and then solved for the natural frequencies and mode shapes of the structure. Available documentation states that Abaqus welds any nodes that are in contact at the end of the static preload step and therefore these nodes are welded during the subsequent linear modal analysis step.

For both the 2D and later 3D models, the first bending mode, forced in Fig. 2, was extracted and was the focus of further analysis. The first 10 modes were requested from the eigenvalue solver so that later examinations for mode coupling could be performed.

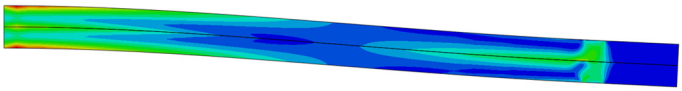

Figure 2. Von Mises stress distribution on 2D model resulting from a static load in shape of Mode 1.

Once the first mode shape was extracted, the shape of the load in Eq. (4) was determined. The load magnitude was specified by giving a desired vertical tip deflection at the free end of the structure. This displacement value was then translated to a maximum forcing amplitude that would scale the forced mode shape to yield the specified tip deflection at the final analysis step. This force magnitude was then applied in the shape of the specified mode, Mode 1 in this case, and was mapped into the modal domain using Eq. (5) and (6). An Abaqus input file was written to apply this force with stabilization and nonlinear geometry settings enabled. This input file was then solved and Fig. 2 shows the resulting stresses and deflection in the shape of Mode 1. Note that as the beam experiences loading, Abaqus evaluates the specified contacting elements as either "sticking" or "slipping" and allows the elements to evolve between the two as the jointed beams experience and increasing force in the shape of Mode 1.

Since mode shapes vary minimally with load amplitude, especially at the smaller forces used for quasi-static analysis, there was no need to recalculate or evaluate mode shapes as the force amplitude increased. This assumption was later justified by examining modal coupling, and is also one difference between Festjens et al.'s method and the implementation of Allen et al.'s method that is used here.

Results from this quasi-static analysis were requested at 50 points, where the user specifies the total number of extracted points, or steps, in the Matlab script that guides the full quasi-static modal analysis of the model. These results were then imported back to Matlab where Masing's assumptions were applied as given in Eq. (7) to create a hysteretic response curve. The supplied forces and displacements, in addition to the quasi-static modal analysis' results, were subdivided into the requested 50 steps and were used for plotting and analysis of the joint damping.

The force displacement curve was almost entirely linear so the linear stiffness was subtracted from the plot as given in Eq. (11), leaving a plot of only the nonlinear portion of the hysteresis curve, shown in Fig. 3. The energy dissipation was then calculated from the full hysteresis curve using the trapezoidal rule from which Eq. (10) was used to calculate the damping ratio that the structure would have when vibrating in this mode. Then the secant of the hysteresis curve was used in Eq. (8) to determine the natural frequency as a function of amplitude. The resulting damping ratios and natural frequencies are plotted versus the peak modal velocity amplitude in Fig. 4. The peak modal velocity is calculated by multiplying the modal velocity (velocity of the modal coordinate, as in [25]) by the mode shape at the point where the deflection is largest.

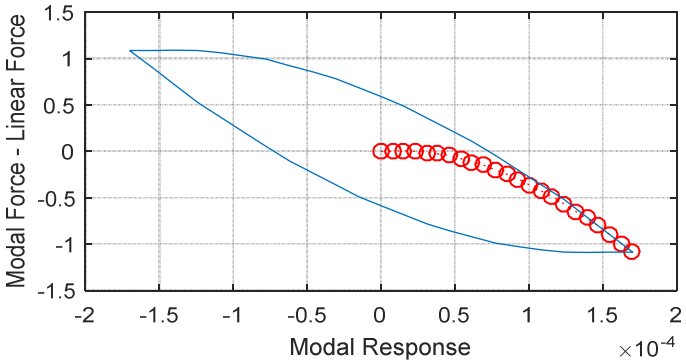

Figure 3. Nonlinear portion of the force-displacement curve (red circles) from which Masing's rules were used to obtain the complete hysteresis curve, shown in blue.

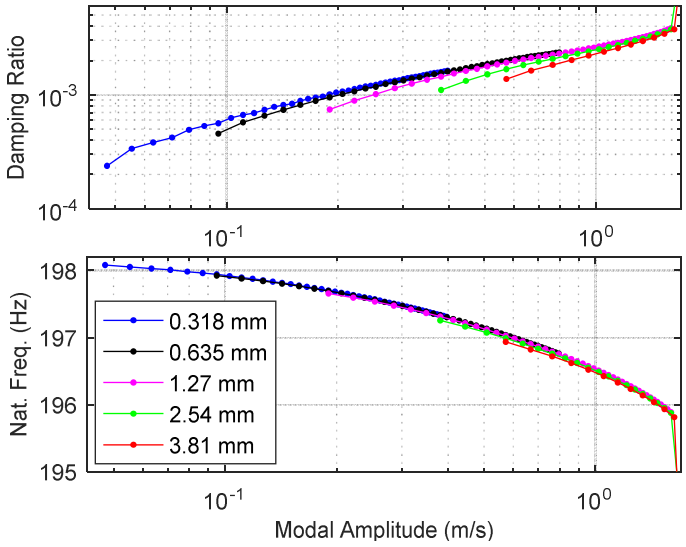

Figure 4. Overlay of 2D model results from different forcing magnitudes as specified by the tip deflection of an equivalent linear model.

In Fig. 4, where each colored line corresponds to forcing the 2D model into the same shape of Mode 1, but with different specified maximum tip deflection values, (i.e. 0.127 mm [0.005 in] means that a force was applied that would produce a tip deflection of 0.127 mm for the linearized model). Various force magnitudes were analyzed since the complete microslip regime needed to be captured to understand the full damping behavior of the joint.

Each analysis at a specified forcing magnitude took approximately 5 minutes on a 4GHz Intel i7 computer using three cores. A significant portion of the time was spent writing the results to a file, since for this implementation the displacement at each node had to be written to file and imported into Matlab.

A few key conclusions can be drawn from Fig. 4. First, at the lowest examined forcing magnitudes, the damping ratio begins near 0.01%, which is likely a value below the material damping threshold, and is therefore unimportant since this behavior would not be observed in practice. The damping ratio then increases with amplitude in a power-law fashion up to about 0.2% at the highest amplitudes considered. Additionally, upon examining the natural frequency plot, the lowest forcing magnitudes gave an initial natural frequency around 198 Hz. This is in agreement with the first mode found by the eigensolver at 198.14 Hz, which therefore confirms the accuracy of the stiffness in the quasi-static model.

Furthermore, the sharp increase in the damping ratio and drop of the natural frequency at higher peak velocities, corresponding to greater forcing magnitudes, signifies the beginning of macroslip; at that force level the quasi-static procedure will typically no longer give a meaningful result.

Lastly, mode coupling was examined to ensure that only the first bending mode was excited by the quasi-static modal analysis. This was done by computing the modal displacement of each of the first five modes at each load step using Eq. (5) and then dividing these displacements by that of the first mode. Hence, Mode 1 always had a magnitude of one and all other modes should have been several orders of magnitudes smaller if they were not strongly coupled to Mode 1. Figure 5 gives a plot of these mode comparison values for the 0.635 mm loading case in Fig. 4. It should be noted that these curves were nearly identical for all loading cases examined.

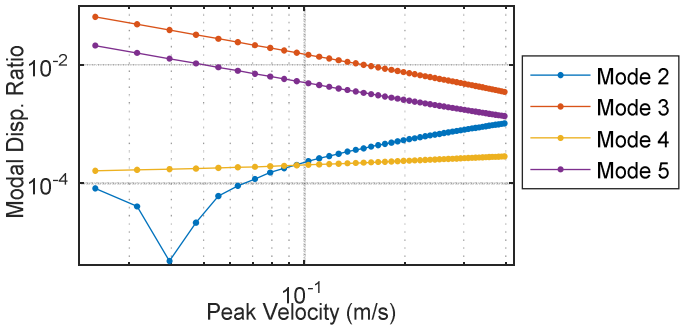

Figure 5. Modal excitations for modes 2 through 5 with a maximum forcing magnitude corresponding to a tip deflection of 0.127 mm.

Mode 3 has a displacement that is 10-100 times smaller than that of Mode 1, and the other modes are excited even less; this confirms that Mode 1 is dominant. It is interesting to note that modes 3 and 5 have contributions that are nonzero at small amplitude and decrease as forces on the model increase; this suggests a possible inaccuracy in the linearized modes of the system computed by Abaqus; there seems to be some difference between the true modes of the nonlinear, clamped beam and the linearized model that Abaqus uses to compute the modes. In general though, all modes are excited to a sufficiently low level in proportion to the bending mode so the re-evaluation of the bending mode shape with changes in forcing amplitudes is proven unnecessary.

Examination of Mesh Convergence, Coefficient of Friction, and Bolt Preload

A mesh convergence study was performed to determine the ideal mesh for all further analyses. New meshes were first produced in Abaqus, then analyzed with the quasi-static modal analysis method, from which the damping ratios and natural frequencies were determined. These results were then overlaid with existing data from Fig. 4 and this process was repeated until a revised mesh remained in agreement with the expected nonlinear effects experienced by the joint during microslip. Ideally, the revised mesh will contain fewer elements and nodes than the original mesh which will save computation time.

The initial mesh was thought to be finer than needed so the new meshes were made increasingly coarse. Convergence was determined by finding the first coarse mesh that produced erroneous damping ratio and natural frequency plots, then selecting the mesh one iteration prior whose results remained in agreement with the expected plots. Over twenty different meshes were analyzed and the mesh over the bolted joint region

experiencing slip is shown for three of those cases in Fig. 6. The first mesh, Mesh A, was the original mesh for which results were shown in Fig. 3-5. The second mesh, Mesh B, had element biasing and the final mesh, Mesh C, was meshed similar to what would be deemed necessary for a basic stress analysis. Table 1 compares node and element counts for each.

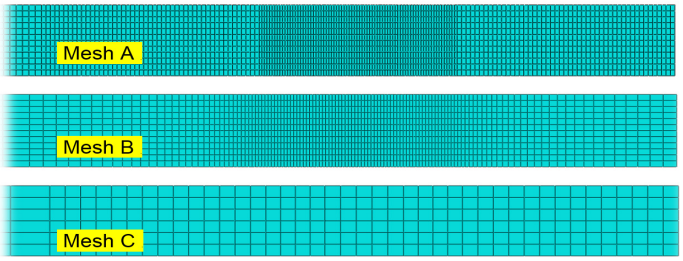

Figure 6. A close up view of a single beam in the 2D model, showing only the bolt region with various meshes.

Table 1. Total node and element count comparisons between 2D model meshes.

Mesh Name	Node Count	Element Count
A	6188	5688
B	4342	3984
C	994	840

Plots overlaying the results from the original Mesh A with results from Mesh B and C are provided in Fig. 7. Mesh C produced results that do not agree with the others, confirming that this mesh was too coarse, while Mesh B's results agree well. Thus Mesh B was used for all remaining 2D analyses and was the basis for the 3D model when it was later constructed. Notice that, at very low amplitudes, Mesh A gives a very small damping ratio indicating that no elements are slipping. For Mesh C this happens at a higher amplitude, and perhaps this feature can be used to gauge whether a mesh is adequately refined.

Two case studies were performed to examine how bolt preload and the coefficient of friction impacted the damping ratio and natural frequency of the jointed structure; the magnitude of bolt preload was first examined. The frequency and damping of the structure were found for various preloads and the results are shown in Fig. 8. Note the apparent choppiness of the lines arises from the parsing together data from several forcing magnitudes. From this figure, it is evident that doubling the preload to 576 Nm [5092 lb-in] on each surface resulted in only a 35% decrease in the damping ratio. The joint does go into macroslip at higher velocity amplitudes, or equivalently, when higher forces are applied to the structure. There was also a small increase in the natural frequency, which is logical since a tighter bolt increases the contact area and hence the stiffness of the joint. Conversely, applying half the original preload, 144 Nm [1273 lb-in] on each surface, caused an approximate 40% increase in the damping ratio and slip was initiated at lower amplitudes. This is a significant finding; increasing or decreasing the preload by a factor of two caused damping to decrease by less than a factor of two, and may explain why joint nonlinearity cannot be removed from a FEA model by simply tightening the bolts.

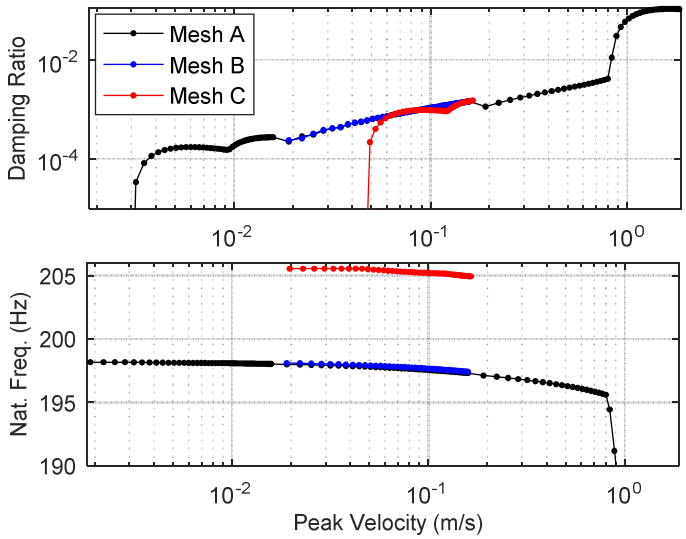

Figure 7. Overlay results for Mesh A with specified tip displacements of 0.0127 mm, 0.127 mm, and 1.27 mm with Mesh B and C both with specified 0.127 mm tip deflection.

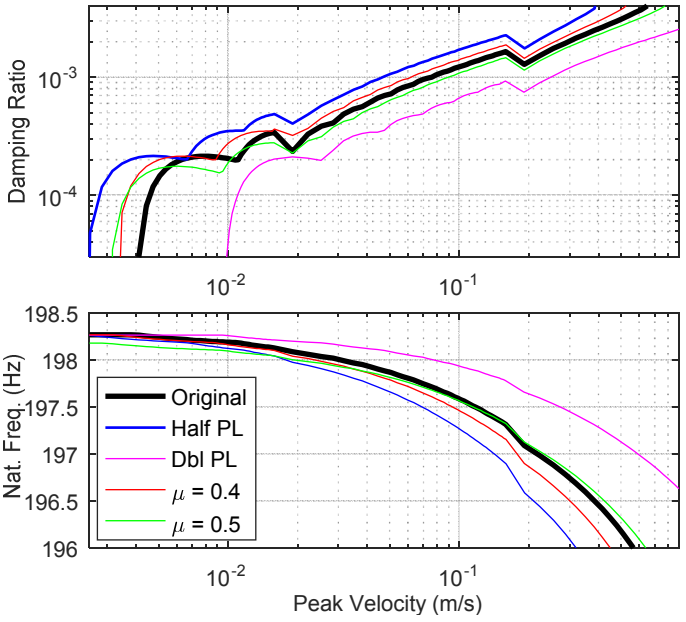

Figure 8. Overlay plots showing results for varying either bolt preloads or coefficients of friction.

Lastly, the coefficient of friction was altered to examine its impact on the natural frequency and damping ratio. Figure 8 also provides plots after altering the coefficient to $\mu = 0.5$ and $\mu = 0.4$. From these plots it can be seen that decreasing the coefficient to $\mu = 0.5$ increased the damping ratios by about 13% and resulted in a slight decrease in natural frequency near macroslip. Decreasing the damping ratio to $\mu = 0.4$ increased the damping ratio from the original coefficient's results by 31% and yielded a slightly larger decrease in natural frequency.

In comparing both modeling parameters and their impacts on the extracted damping ratios and natural frequencies, it is

found that varying the coefficient of friction resulted in smaller changes towards both curves than varying the preload of the bolt. Therefore if a more dramatic shift of both the damping ratio and the natural frequency is desired, while maintaining a consistent initial natural frequency value, the bolt preload should be the parameter altered.

APPLICATION TO 3D MODEL

Finite Element Model Creation

While the 2D model provides interesting insights, the ultimate goal of this work is to predict the stiffness and damping of real joints and to compare results from the quasi-static modal analysis method with measurements. Hence, a 3D model for the same bolted joint structure was also constructed and analyzed. With lessons learned from the 2D modeling process, the mesh for the 3D model was more efficiently created. Similar to the 2D model, each beam was 203 mm [8 in] long, 6.35 mm [0.25 in] thick, and 50.8 mm [2 in] wide. The single bolt was located 25.4 mm [1 in] from the free end of the beam (the opposite end had fixed boundary conditions on both beam faces), identical to what was done for the 2D model. Unlike the 2D model though, the bolt was physically represented and was modeled after a standard 6.35 mm [0.25 in] diameter bolt with two washers and a nut. The geometry of both the beam and bolt are shown in Fig. 9. The mesh for all parts in the assembly, as seen in Fig. 10, was composed of C3D8 elements and had the same steel material properties used for the 2D model.

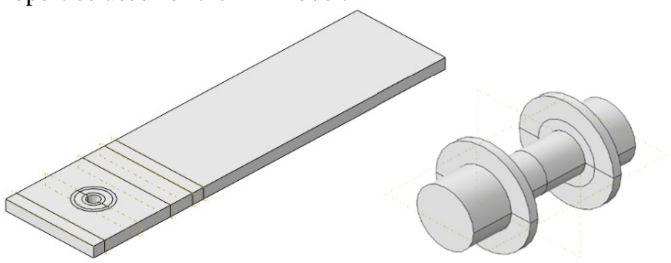

Figure 9. Geometry of beam and bolt for 3D model.

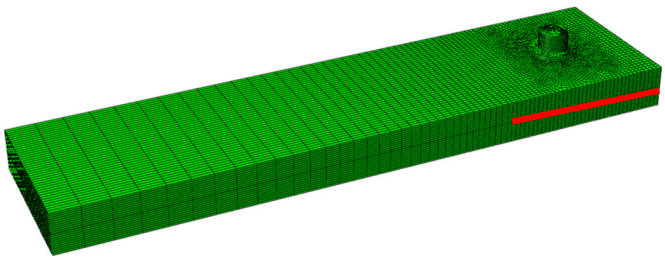

Figure 10. Finite element model of 3D cantilever stacked beams with bolt. Face-to-face contact enabled in the region shown by a red line.

For the 3D model, contact was enabled in three distinct regions: between the two beams in the 50.8 mm by 50.8 mm [2 in. by 2 in.] region surrounding the bolt, and between the outer beam surfaces and the corresponding top or bottom of the washers. When meshing, special consideration was taken to ensure that all nodes in these contact regions were aligned between the master and slave surfaces. Additionally, nodes along the bolt shaft and holes of each beam were aligned. Similar to the 2D modeling procedure, the coefficient of friction for all of the contact regions was set to $\mu = 0.6$ and Lagrange tangential behavior with hard contact (Penalty) normal behavior were selected. Abaqus nonlinear geometry and solution stabilization was also enabled similar to 2D.

To preload the bolt, a "Bolt Load" was applied in Abaqus. This required splitting the bolt geometry in two and selecting the mid-plane face as the cross section of the bolt. Then the axis of the bolt was defined and lastly the force on the bolt was specified as 1000 lb (4450 N). The final assembly mesh contained 158,798 nodes and 139,900 elements.

Quasi-static Analysis Results

The same analysis process was carried out on the 3D model as was done on the 2D model. A hysteresis curve of the modal force with respect to response was created, similar to Fig. 4. From this curve, damping ratios and natural frequencies were extracted to produce plots of these parameters versus peak velocity. A variety of quasi-static load amplitudes were applied to the 3D model to capture results throughout the microslip regime and these plots are overlaid in Fig. 11. Attempts for 0.635 mm [0.025 in] vertical tip deflection and greater failed to converge.

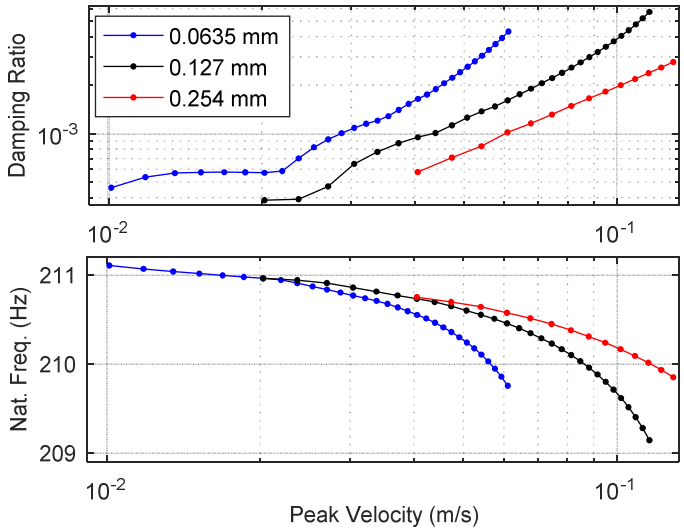

Figure 11. Overlay of 3D model results from different forcing magnitudes specified by tip deflection in legend.

Upon first examination of Fig. 11, the curves corresponding to various forcing levels display unexpected results. Since only the forcing magnitude, or load level, was altered, one would expect all of the curves to show a portion of the same either damping versus amplitude curve (top Fig. 11) or frequency versus amplitude curve (bottom Fig. 11), similar to the 2D model results in Fig. 13. Instead, Fig. 11 gives illogical physical results, suggesting a non-consitent natural frequenccy with regard to forcing, and therefore the 3D model needed to be modified to

yield expected results. Additionally, all plotted load cases in Fig. 11 failed to converge to the final desired forcing magnitude or end tip displacement. Therefore, due to it's nonconverging solutions and physicaly unreasonable results, the 3D model was reevaluated with different stabilization settings as well as contact formulations.

Examining Abaqus Stabilization and Contact Formulation Selections

Several combinations of Abaqus' stabilization and contact formulations were evaluated and are documented in Table 2. Plots of the cases from the first five rows, where both the stabilization was changed to contact stabilization and different contact formulations were selected, can be seen in Fig. 12. All curves are results from quasi-static modal analysis with a load specified to produce 0.127 mm [0.005 in] tip displacement.

Table 2. Trial cases for 3D model with various contact formulations and stabilization settings.

Name	Tangential Contact	Slip tolerance Tolerance	Normal Contact	Stabilization
A	Lagrange	N/A	Penalty	ALLSDTOL = 0
B	Lagrange	N/A	Penalty	Contact
C	Lagrange	N/A	Lagrange	Contact
D	Penalty	5e-3	Penalty	Contact
E	Penalty	5e-4	Penalty	Contact
F	Penalty	5e-4	Penalty	ALLSDTOL = 0
G	Penalty	1e-5	Penalty	ALLSDTOL = 0
H	Penalty	1e-6	Penalty	ALLSDTOL = 0

Figure 12 immediately reveals that contact stabilization regardless of the contact formulation employed gave spurious stiffness and damping at low load levels in Fig. 12. As the load increased however, more reasonable results were attained. It appears that the contact stabilization algorithm introduces spurious forces that contaminate the results for small loads but eventually seem to disappear as the highest load levels are reached. In any event, by turning off the adaptive part of the stabilization by using ALLSDTOL=0, this problem was avoided. Furthermore, the contact stabilization algorithm did not seem to converge to significantly higher force levels than the basic approach and so there was no need to pursue that further.

Different contact formulations were examined because of the Lagrange formulation's failure to converge in the previous 3D model. The Lagrange method is preferred since it consistently produces physically realistic results, however, it was not possible to solve the problem up to the desired load levels using that approach. Therefore, penalty formulations were also examined, as documented in Table 2, and results were compared with those from Lagrange methods.

Changing to a Penalty tangential contact formulation requires specifying a maximum slip tolerance (called "Slip tolerance in the GUI), which Abaqus uses to calculate stick and slip behavior. The default value was 0.005 but several other values were also analyzed, see Table 2. Revisiting the results depicted in Figure 12, the Lagrange curves (Case B and C) took approximately 24 hours while the Penalty method curves (Case D and E) took approximately 6 hours suggesting a significant cost benefit. Furthermore, the penalty formulations converged over the whole range of loads that was desired penalty. These simulation times are from computation on a 4GHz Intel i7 computer using two cores.

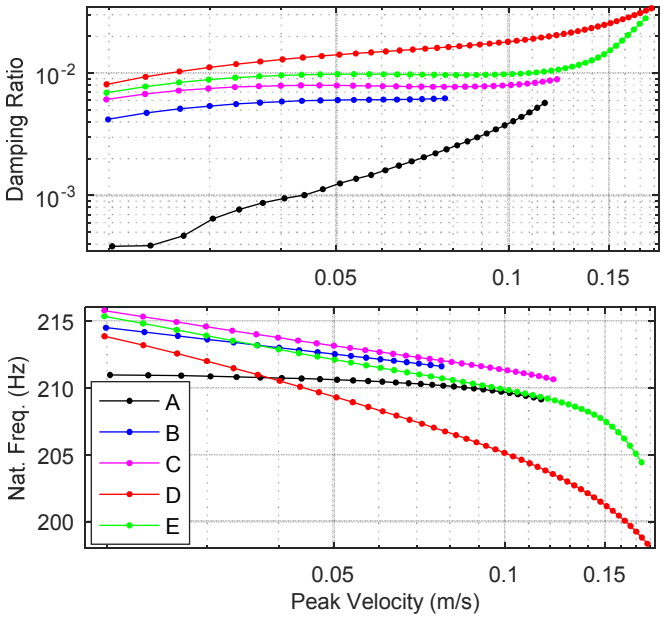

Figure 12. Results for 3D Model at 0.127 mm tip displacement for various cases as denoted in Table 2.

However, the Penalty method curves depicted in Fig. 12 are still in disagreement with expected results so the slip tolerance was further decreased by several orders of magnitude, as documented in Table 2 and these results are given in Fig. 13.

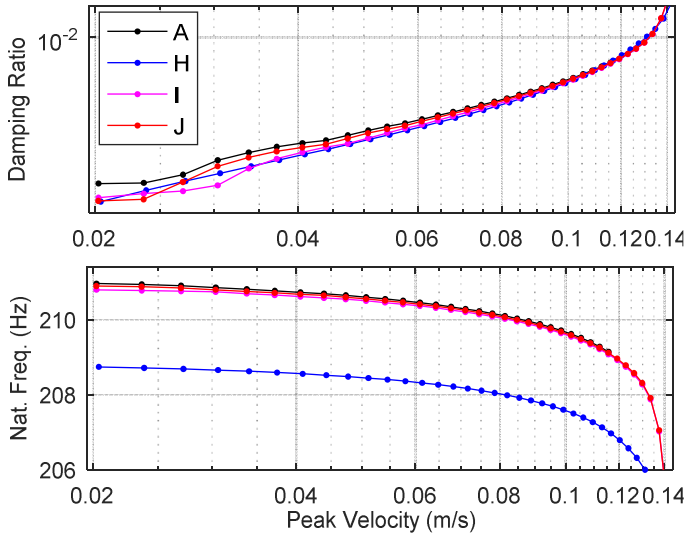

Figure 13. Results for 3D Model at 0.127 mm tip displacement for various cases as denoted in Table 2.

This figure shows that as the slip tolerance decreases, the tangential Penalty method converges to the Lagrange solution

which was originally plotted in Fig. 11. Case H with a slip tolerance at 1e-6 gave results in best agreement with the original results from Fig. 11, and is therefore plotted against these results in Fig. 14 at various forcing magnitudes. However, whereas the computation time was significantly reduced when using the penalty method with a large slip tolerance, computation time for Case H, which used the Penalty method with a tight tolerance, was approximately 22 hours, so the time savings was not as significant but at least the Penalty method was able to converge over the entire range of load levels. It is therefore concluded that a tangential Penalty formulation with a low slip tolerance, approximately 1e-5 or 1e-6 for this model, and stabilization with ALLSDTOL = 0, gives repeatable, consistent, convergent results for quasi-static modal analysis of a 3D model.

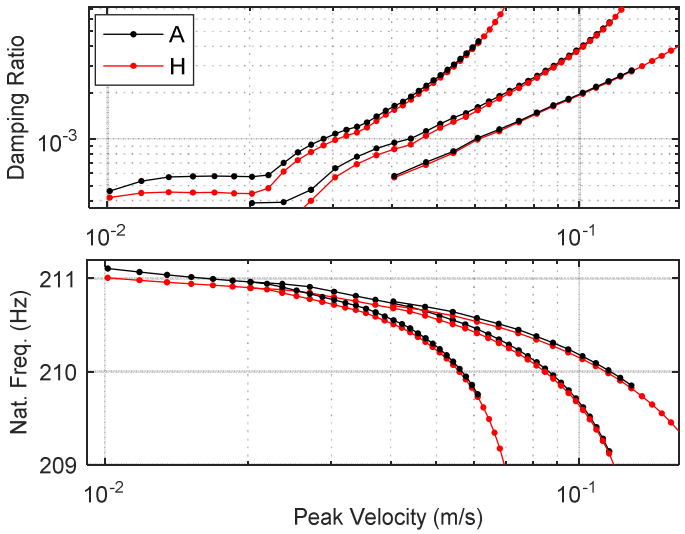

Figure 14. Results for 3D Model versions A and H from Table 2 at various forcing magnitudes corresponding to specified tip displacements 0.0635 mm (left), 0.127 mm (center), and 0.254 mm (right).

The results in Fig. 14 show agreement between the penalty and Lagrange formulations, and the former was able to continue the solutions to higher force levels. However, these results still do not seem to make sense physically. The results suggest that as the final load increases, that the stiffness of the joint decreases at the same displacement level. There seems to be no physical justification for this behavior; both models begin at the same equilibrium state and the load increases monotonically so one would expect the stiffness to decrease identically. Similarly, the results suggest that the damping produced by the joint also increased with the magnitude of the final load. At the time of this writing, the authors are unable to explain these phenomenon, and are seeking to understand what defect they might point to in the tolerances used, the solution procedure requested or in Abaqus' contact solver.

CONCLUSIONS

While it is still expensive, this work has shown that quasi-static modal analysis appears to be tractable when modeling joints in detail. To date, 2D models have given reasonable results with the expected trends in damping ratio and natural frequency when a Lagrange formulation is used for tangential contact. This Lagrange method was compared with Abaqus' default penalty method and resulted in similar results in 2D but not 3D.

While the 2D models do not capture the joints of interest accurately, it was extremely helpful to study the 2D model first, because it was easy to create and mesh. Furthermore, analysis times were on the order of minutes which allowed for easy examination of a variety of contact and model parameters. Results showed that the most important consideration for accurately capturing dissipation at the joint was the finite element mesh size. Brink [22] had suggested a somewhat denser element mesh than was required for the structure studied here; for this system it seems that the mesh near the bolt should be modeled in 2D by 11.8 elements per mm along the contacting interface. In 3D, the region near the bolt should be modeled using 2 elements per mm circumferentially, 2.11 elements per mm radially up to the outer washer radius, and 1.57 elements per mm along the bolt shaft.

The 2D bolted joint model also provided a basis for examining the effect of varying either the bolt preload or the coefficient of friction at contacting surfaces on the effective damping ratio and natural frequency of the model. The bolt's preload was shown to have a more dramatic effect than the coefficient of friction. Changes to either of these parameters yielded expected and physically reasonable shifts of the damping ratio and natural frequency curves, suggesting that the quasi-static analysis method is effective for 2D models.

In 3D, when the Lagrange method was used for tangential contact the algorithm failed to converge. It was found that changing to a tangential Penalty method formulation, and reducing the slip tolerance from the default 0.05 to 1e-5 or 1e-6 gave results that seemed to agree with the Lagrange method. Conclusively, it seems advisable for 3D models to follow this pattern for selecting contact formulations wherein first, the Lagrange method is used to obtain truth data (possibly only at lower force levels) and then changing to a Penalty method and progressively reducing the slip tolerance until comparable results are obtained.

Lastly, in the cases studied here we found that adaptive stabilization, such as is used in the default "contact stabilization" algorithm in Abaqus, added spurious stiffness and damping to the solutions at lower load levels. This can be circumvented by using the standards stabilization with ALLSDTOL = 0.

Unfortunately, even after all of these studies and many, many hours of computation time, we were still unable to obtain physically reasonable results for the 3D model. Future studies will seek to address this issue. Furthermore, dynamic measurements will be acquired form a similar structure this summer during the 2017 Sandia Nonlinear Mechanics and Dynamics (NOMAD) summer institute, and the effective damping and natural frequency can be extracted from these measurements to determine whether this model gives quantitatively accurate results.

ACKNOWLEDGMENTS

This material is based in part upon work supported by the National Science Foundation under Grant Number CMMI-1561810. Any opinions, findings, and conclusions or recommendations expressed in this material are those of the author(s) and do not necessarily reflect the views of the National Science Foundation.

REFERENCES

[1] Ibrahim, R. A., and Pettit, C. L., 2005, "Uncertainties and dynamic problems of bolted joints and other fasteners," Journal of Sound and Vibration, 279(3-5), pp. 857-936.

[2] Kim, J., Yoon, J.-C., and Kang, B.-S., 2007, "Finite element analysis and modeling of structure with bolted joints," Applied Mathematical Modelling, 31(5), pp. 895-911.

[3] Petrov, E. P., and Ewins, D. J., 2003, "Analytical Formulation of Friction Interface Elements for Analysis of Nonlinear Multi-Harmonic Vibrations of Bladed Disks," Journal of Turbomachinery, 125(2), pp. 364-371.

[4] Salles, L., Swacek, C., Lacayo, R. M., Reuss, P., Brake, M. R. W., and Schwingshackl, C. W., 2015, "Numerical Round Robin for Prediction of Dissipation in Lap Joints," 33rd International Modal Analysis Conference (IMAC XXXIII), Springer, Orlando, Florida.

[5] Segalman, D. J., 2005, "A Four-Parameter Iwan Model for Lap-Type Joints," Journal of Applied Mechanics, 72(5), pp. 752-760.

[6] Segalman, D. J., Gregory, D. L., Starr, M. J., Resor, B. R., Jew, M. D., Lauffer, J. P., and Ames, N. M., 2009, "Handbook on Dynamics of Jointed Structures," Sandia National Laboratories, Albuquerque, NM 87185.

[7] Smith, S., Bilbao-Ludena, J. C., Brake, M. R., Reuss, P., and Schwingshackl, C. W., 2015, "The Effects of Boundary Conditions, Measurement Techniques, and Excitation Type on Measurements of the Properties of Mechanical Joints," 33rd International Modal Analysis Conference (IMAC XXXIII)Orlando, Florida.

[8] Festjens, H., Chevallier, G., and Dion, J.-L., 2013, "A numerical tool for the design of assembled structures under dynamic loads," International Journal of Mechanical Sciences, 75, pp. 170-177.

[9] Allen, M. S., Lacayo, R., and Brake, M. R. W., 2016, "Quasi-static Modal Analysis based on Implicit Condensation for Structures with Nonlinear Joints," International Seminar on Modal Analysis (ISMA)Leuven, Belgium.

[10] Beards, C. F., 1979, "Damping in Structural Joints," The Shock and Vibration Digest, 11(9), pp. 35-41.

[11] Rooke, D. P., and Edwards, P. R., 1988, "Waveforms in Fretting Fatigue," Fatigue & Fracture of Engineering Materials and Structures, 11(6), pp. 447-465.

[12] Gaul, L., and Lenz, J., 1997, "Nonlinear dynamics of structures assembled by bolted joints," Acta Mechanica, 125(1-4), pp. 169-181.

[13] Hartwigsen, C. J., Song, Y., McFarland, D. M., Bergman, L. A., and Vakakis, A. F., 2004, "Experimental study of non-linear effects in a typical shear lap joint configuration," Journal of Sound and Vibration, 277(1-2), pp. 327-351.

[14] Menq, C. H., Bielak, J., and Griffin, J. H., 1986, "The influence of microslip on vibratory response, part I: A new microslip model," Journal of Sound and Vibration, 107(2), pp. 279-293.

[15] Roettgen, D. R., and Allen, M. S., 2016, "Nonlinear characterization of a bolted, industrial structure using a modal framework," Mechanical Systems and Signal Processing, In Press.

[16] Segalman, D. J., 2006, "Modelling joint friction in structural dynamics," Structural Control and Health Monitoring, 13(1), pp. 430-453.

[17] Ungar, E. E., 1973, "The status of engineering knowledge concerning the damping of built-up structures," Journal of Sound and Vibration, 26(1), pp. 141-154.

[18] Liu, Y. F., Li, J., Zhang, Z. M., Hu, X. H., and Zhang, W. J., 2015, "Experimental comparison of five friction models on the same test-bed of the micro stick-slip motion system," Mechanical Sciences, 6(1), pp. 15-28.

[19] Pennestrì, E., Rossi, V., Salvini, P., and Valentini, P. P., 2015, "Review and comparison of dry friction force models," Nonlinear Dynamics, 83(4), pp. 1785-1801.

[20] Sun, Y.-H., Chen, T., Qiong Wu, C., and Shafai, C., 2015, "Comparison of Four Friction Models: Feature Prediction," Journal of Computational and Nonlinear Dynamics, 11(3), p. 031009.

[21] Vodička, R., Mantič, V., and Roubíček, T., 2017, "Quasistatic normal-compliance contact problem of visco-elastic bodies with Coulomb friction implemented by QP and SGBEM," Journal of Computational and Applied Mathematics, 315, pp. 249-272.

[22] Brink, A. R., 2015, "Modeling Complex Contact Phenomena with Nonlinear Beamshells,"Thesis.

[23] Krack, M., Bergman, L. A., and Vakakis, A. F., 2016, "On the efficacy of friction damping in the presence of nonlinear modal interactions," Journal of Sound and Vibration, 370, pp. 209-220.

[24] Schwingshackl, C. W., Maio, D. D., Sever, I., and Green, J. S., 2013, "Modeling and validation of the nonlinear dynamic behavior of bolted flange joints," Journal of Engineering for Gas Turbines and Power, 135(12).

[25] Lacayo, R., Deaner, B., and Allen, M. S., 2017, "A Numerical Study on the Limitations of Modal Iwan Models for Impulsive Excitations," Journal of Sound and Vibration, Accepted Nov 2016.

